

NASA TECHNICAL NOTE



NASA TN D-2126

C.1

**LOAN COPY: RETURN
AFWL (WLL—)
KIRTLAND AFB, N M**

0154400



TECH LIBRARY KAFB, NM

NASA TN D-2126

**NUMERICAL PREDICTIONS OF
NONLINEAR DIFFUSION WITH
HOMOGENEOUS RECOMBINATION AND
TIME-VARYING BOUNDARY CONDITIONS**

by Walter A. Reinhardt

Ames Research Center

Moffett Field, California

NUMERICAL PREDICTIONS OF NONLINEAR DIFFUSION WITH
HOMOGENEOUS RECOMBINATION AND TIME-VARYING
BOUNDARY CONDITIONS

By Walter A. Reinhardt

Ames Research Center
Moffett Field, Calif.

NATIONAL AERONAUTICS AND SPACE ADMINISTRATION

For sale by the Office of Technical Services, Department of Commerce,
Washington, D.C. 20230 -- Price \$1.00



NUMERICAL PREDICTIONS OF NONLINEAR DIFFUSION WITH
HOMOGENEOUS RECOMBINATION AND TIME-VARYING
BOUNDARY CONDITIONS

By Walter A. Reinhardt

SUMMARY

A numerical method is developed to determine the periodic solution of a nonlinear partial differential equation with unsteady boundary conditions. More specifically, the analysis treats the unidimensional, time-varying diffusion equation with a nonlinear sink term. The equation that is solved follows from a suggested experiment whereby the homogeneous recombination and diffusion rates of oxygen atoms are determined by studying the spatial decrease of the amplitude of the time variation in concentration of atoms. In the numerical method, the partial differential equation and boundary conditions are approximated by a set of difference equations that are then solved on an electronic computer. An initial condition that is not specifically known is required in the numerical procedure. It is shown that an arbitrary choice for the initial condition merely produces a transient that decays as the time variable increases in value. The remaining solution is periodic and independent of the initial condition. Iso-metric plots, obtained from an automatic plotter, show the effect of the transient on the solution. The periodic solution characterized by a set of upper and lower envelopes, within which the concentration varies, is also illustrated by curves from an automatic plotter. To study the functional dependence of the envelopes on the frequency of the concentration variation and on the sink term coefficient, a new variable, called the penetration depth, is introduced to relate the difference in values between the upper and lower envelopes to the frequency and sink term coefficient. A discussion is included on the use of the penetration depth curves in a proposed experiment to determine the recombination and diffusion rate constants. Discussion is also included on the accuracy of the numerical method and on a linearized sink term approximation to the nonlinear partial differential equation.

INTRODUCTION

In the present report a numerical solution is given for the nonlinear problem of unsteady diffusion in a ternary mixture of diatomic molecules, dissociated atoms, and an inert gas. The problem follows from a suggested experiment (see ref. 1) whereby the homogeneous reaction and diffusion rates of oxygen atoms can be determined from the decay of the time variation in concentration of atoms. In the proposed experiment a periodic concentration of atoms is formed by dissociation at one end of a test cell. The atoms diffuse into the test cell and recombine, thereby providing a time-varying supply of freshly recombined molecules throughout the cell. Associated with this process is a decrease in

the amplitude of concentration variation from the inlet end of the test cell to the opposite end. This decrease depends on the oscillation frequency of the concentration and is, in part, due to the loss of atoms in the recombination process. To interpret the data obtained from such an experiment, a relation is required for the dependence of the amplitude decrease on the frequency and on the recombination rate. To this end, a periodic solution of the unsteady multicomponent diffusion equation is needed. The equation that describes the process is derived in reference 1. To lowest order the equation is linear except for a sink term, which represents the atom recombination process. A closed-form solution is not available for such an equation. Therefore, to gain a qualitative understanding of the problem the nonlinear sink term was first linearized (in ref. 1). A closed-form solution was then obtained from the linearized equation. In the present report a numerical solution is found for the equations with the sink term in its nonlinear form.

NOTATION

D_{ij}	binary diffusion coefficient for species i and j
D	characteristic diffusion constant, $\left(\frac{D_{23} \phi_1}{\phi_2 D_{13} + \phi_3 D_{12}} \right) \frac{D_{12} D_{13}}{D_{23}}$
E	decay fraction (see eq. (17))
$F(\phi, C)$	incomplete elliptic integral of the first kind with argument ϕ and modulus C
h	stability relation, $\frac{\Delta \tau}{(\Delta \xi)^2}$
K_r	recombination rate constant
k_r	dimensionless nonlinear sink strength, $\left(\frac{L^2}{D} \phi_1 \phi_2 \phi_3 \right) K_r$
k_r'	dimensionless linear sink strength, $\left(\frac{L^2}{D} \phi_1 \phi_2 \phi_3 \right) K_r'$
L	characteristic length appearing in dimensionless coordinate
N	total number of points in grid defining length L
n_i	number density for species i
$n(o)$	number density defined on inlet plane
ϕ_0	zero-order number density, $\phi_2 + \phi_3$
W	dimensionless frequency, $\frac{L^2 \omega}{D}$
Z	coordinate variable measuring distance from inlet plane
λ	dimensionless perturbation parameter (see eq. (4e) and discussion following that equation)

ϵ_n^J	transient magnitude (see eq. (15))
$\mu(\xi, \tau)$	dimensionless atom concentration, $\frac{n_1}{n_0}$
μ_n^m	dimensionless atom concentration that is a numerical approximation to $\mu[(n-1)\Delta\xi, (m-1)\Delta\tau]$
$\bar{\mu}$	average value of $\mu(\xi, \tau)$
$\mu_{\max}(\xi)$	maximum value of $\mu(\xi, \tau)$ with respect to time
$\mu_{\min}(\xi)$	minimum value of $\mu(\xi, \tau)$ with respect to time
ξ	dimensionless coordinate variable, $\frac{Z}{L}$
ξ_E	penetration depth corresponding to decay fraction E (see eq. (19))
τ	dimensionless time variable, $\frac{Dt}{L^2}$
ω	angular frequency

Subscripts

i	species kind
n	grid number corresponding to variable ξ
1	atoms
2	molecules
3	inert gas

Subscript o appearing before a symbol indicates zeroth order in terms of an expansion with respect to λ (see eq. (11), ref. 1)

Superscript

m	grid number corresponding to variable τ
-----	--

ANALYSIS

In the following two sections the equations given are those required to obtain the solution for the problem of diffusion and recombination with time-varying boundary conditions. In the first section the pertinent equations

derived in reference 1 are reviewed. These equations apply to a one-dimensional system where diffusion and recombination occur with zero stream velocity in a region between two infinite planes and where the species concentration is varied on the inlet plane. This specialization also presupposes that reactions on the far boundary plane are negligible. A closed-form solution for these equations is not available; therefore, recourse is made to numerical methods. In the second section, the numerical methods that are used to obtain the solution are described. Here the diffusion equation and boundary conditions are approximated by a set of difference equations. The difference equations are then put into a form suitable for programming on an electronic computer.

Basic Equations

The basic equations to be solved were derived in reference 1. In this reference the general multidimensional differential equation for atom concentration is given by equation (54a). Discussion will be limited in this report to zero stream velocity in a one-dimensional system representing diffusion between two parallel planes a unit distance apart. Also, only one term of the double series expansion described in reference 1 will be considered; therefore, the subscripts and superscripts will be dropped. The differential equation then becomes

$$\frac{\partial \mu}{\partial \tau} - \frac{\partial^2 \mu}{\partial \xi^2} = k(\mu) \quad (1)$$

The variables ξ , τ , and μ are dimensionless quantities representing distance from the plane where the atom concentration is being varied (inlet plane), time, and concentration, respectively. The quantity $k(\mu)$ is the sink term resulting from the homogeneous recombination of atoms. The transformation equations that relate the dimensionless quantities to their dimensional equivalents are

$$\mu = \frac{n_1}{n} \quad (2a)$$

$$\xi = \left(\frac{1}{L}\right) Z \quad (2b)$$

$$\tau = \left(\frac{D}{L^2}\right) t \quad (2c)$$

$$W = \left(\frac{L^2}{D}\right) \omega \quad (2d)$$

where W is a dimensionless frequency, Z is the variable measuring distance between the two planes that are separated a distance L apart, and D is a diffusion constant defined by equation (54d) in reference 1; that is,

$$D = \left(\frac{D_{23} \text{on}}{\text{on}_2 D_{13} + \text{on}_3 D_{12}} \right) \frac{D_{12} D_{13}}{D_{23}} \quad (3)$$

The parameters on_2 and on_3 are the zeroth order expressions (see ref. 1) for the fractional number densities of molecular oxygen and the inert gas, respectively. These terms are obtained from an expansion about a uniform state of the gas and therefore are constant.

The total number density is given by $\text{on} = \text{on}_2 + \text{on}_3$. The variable n_1 is the first-order number density of atomic oxygen. The quantities D_{12} , D_{13} , and D_{23} are binary diffusion constants for atomic oxygen and molecular oxygen, atomic oxygen and the inert gas, and molecular oxygen and the inert gas, respectively. The sink term $k(\mu) = -k_r \mu^2$ is given by equation (66a) of reference 1. When the atoms lost by wall reaction are considered negligible compared to those lost in the homogeneous reaction, the problem becomes one of solving the following partial differential equation:

$$\frac{\partial \mu}{\partial \tau} - \frac{\partial^2 \mu}{\partial \xi^2} = k_r \mu^2 \quad (4a)$$

with near wall boundary condition given by

$$\mu(0, \tau) = (1 + \cos W\tau)/2 \quad (4b)$$

and with the far wall boundary condition given by equation (96) of reference 1

$$\left. \frac{\partial \mu}{\partial \xi} \right|_{\xi=1} = 0 \quad (4c)$$

and initial condition given by

$$\mu(\xi, 0) = f(\xi) \quad (4d)$$

where

$$k_r = \left(\frac{L^2}{D} \text{on}^2 \lambda \right) K_r \quad (4e)$$

The number λ is a dimensionless perturbation parameter (see eq. (10), ref. 1) and is defined as the ratio $n_1(0)_{\text{max}}/n(0)$ where $n_1(0)_{\text{max}}$ is the maximum concentration of atomic oxygen and $n(0)$ is the total number density. The zero in

the parentheses indicates that these concentrations are measured on the inlet plane, $\xi = 0$. The constant K_r is defined as the reaction or recombination rate constant and has the dimension $(cc/particle)^2 sec^{-1}$.

Before a solution can be found for equations (4), the initial condition, $\mu(\xi, 0)$, must be specified. The solution of most interest is the periodic solution that results when the time approaches infinity. The exact initial conditions may not be obtainable for this problem. The numerical method used in this report requires that an initial condition be specified. It turns out that the periodic solution is independent of the conditions chosen, but the rate of convergence to the periodic solution does, in fact, depend on the initial conditions specified. This is exemplified later.

Numerical Equations

A simple method that may be used to obtain an approximate solution to equations (4) is that of finite differences. Here the continuum of points in the (ξ, τ) plane over which the independent variables ξ and τ are defined are approximated by a set of discrete points that define a mesh or grid. The partial derivatives for the continuum are then approximated by a set of finite-difference relations expressed in terms of these points. These difference relations yield equations that reduce to a set of nonlinear algebraic equations that can then be solved.

Assume that the mesh size increments are given by $\Delta\xi$ and $\Delta\tau$. The independent variables ξ and τ are expressed in terms of the set of points, denoted by the integers n and m , through the relations

$$\xi = (n - 1)\Delta\xi \quad n = 1, 2, \dots, N \quad (5a)$$

and

$$\tau = (m - 1)\Delta\tau \quad m = 1, 2, \dots \quad (5b)$$

From equation (5a) one notes that

$$\Delta\xi = (N - 1)^{-1} \quad (6)$$

where N is an integer denoting the number of grids between and including the inlet and far boundary planes. The approximation of $\mu[(n - 1)\Delta\xi, (m - 1)\Delta\tau]$ is denoted by μ_n^m . The partial derivatives are approximated in terms of difference relations by the following expressions

$$\frac{\partial \mu}{\partial \xi} \approx \frac{\mu_{n+1}^m - \mu_n^m}{\Delta \xi} \quad (7a)$$

$$\frac{\partial^2 \mu}{\partial \xi^2} \approx \frac{\mu_{n+1}^m - 2\mu_n^m + \mu_{n-1}^m}{(\Delta \xi)^2} \quad (7b)$$

$$\frac{\partial \mu}{\partial \tau} \approx \frac{\mu_n^{m+1} - \mu_n^m}{\Delta \tau} \quad (7c)$$

In terms of these relations, the partial differential equation (4a) becomes

$$\frac{\mu_n^{m+1} - \mu_n^m}{\Delta \tau} - \frac{\mu_{n+1}^m - 2\mu_n^m + \mu_{n-1}^m}{(\Delta \xi)^2} = -k_r(\mu_n^m)^2 \quad (8)$$

The boundary and initial conditions, equations (4b)-(4d), are approximated by

$$\mu_1^m = \frac{1 + \cos [W(m-1)\Delta \tau]}{2} \quad (9a)$$

$$\frac{\mu_N^{m+1} - \mu_{N-1}^{m+1}}{\Delta \xi} = 0 \quad (9b)$$

$$\mu_n^1 = f[(n-1)\Delta \xi] \quad (9c)$$

where

$$n = 1, 2, \dots, N; \quad m = 1, 2, \dots$$

Once $\Delta \xi$, $\Delta \tau$, and f are specified, the problem becomes one of solving simultaneously the above system of algebraic equations. It turns out that the choice of the function f affects the rate of convergence of the solution μ_n^m to the desired periodic solution. This point will be discussed in the next section. The values that are used for $\Delta \xi$ and $\Delta \tau$ affect the accuracy and numerical stability of the solution. One observes first that in the limit as $\Delta \xi$ and $\Delta \tau$ tend to zero, equations (7a) to (7c) are exact expressions for the partial derivatives.

Therefore, one expects that by taking the increments sufficiently small, the numerical solution can be made as accurate as desired. This is correct except that as one increment is reduced the other increment must accordingly be reduced. The spacings between the grids therefore are not independently arbitrary, but are functionally related through a "stability" relation that insures numerical stability. The stability relation for the difference equation, equation (8), is given by

$$h = \frac{\Delta\tau}{(\Delta\xi)^2} \quad (10a)$$

where

$$h \leq \frac{1}{6} \quad (10b)$$

This relation was not derived analytically, but was discovered by trial. The necessity for such a relation, including an analytically determined expression applicable to linear heat or diffusion problems, is discussed in detail in reference 2.

Equations (8) and (9) are not yet in a form adaptable for machine computation. A more desirable form is obtained by rearranging terms in equations (8) and (9b) in such a manner as to obtain the expressions

$$\mu_n^{m+1} = \mu_n^m(1 - 2h) + h(\mu_{n+1}^m + \mu_{n-1}^m) - k_r\Delta\tau(\mu_n^m)^2 \quad (11)$$

and

$$\mu_N^{m+1} = \mu_{N-1}^{m+1} \quad (12)$$

Equations (11), (12), (9a), and (9c) along with a given expression for f are a complete set of numerical equations that may be solved for the dependent variable μ_n^m .

SOLUTION

Before proceeding with the detailed description of the solution, it will be helpful to first describe the nature of the numerical results. Figure 1 shows schematically the pertinent features of the solution. When the value of dimensionless time τ is less than zero, the dimensionless concentration $\mu(\xi, \tau)$ is zero for all values of the spatial coordinate ξ . Since such an initial condition is not an initial condition for the periodic solution, the variation in concentration changes from the initial to the final periodic solution. This transition is referred to here as the transient part of the solution. One observes in figure 1 that the transient part of the solution changes until at a time

corresponding to period number m_s it becomes periodic. From time $\tau_s = m_s(2\pi/W)$ and continuing indefinitely the variation is periodic. The periodic solution $\mu(\xi, \tau)$ when projected on the (μ, ξ) plane shows a variation between a maximum and minimum with respect to time represented by two envelopes. These envelopes indicate that the decrease in the variation in concentration between the inlet and far boundary planes is functionally related to the inlet plane concentration frequency W and the value of the sink term coefficient k_r . The decrease will be characterized by a penetration depth, ξ_E , that is defined as the depth at which the periodic concentration has decayed to some specified fraction of its input value. The dependence of the penetration depth on the parameters W and k_r is then determined. The features of the transient and the periodic parts of the solution described above are discussed in detail in the following two sections.

Solution - Transient Part

The difference equations, equations (11), (12), (9a), and (9c), were programmed for an IBM 7090 electronic computer using two independent sets of initial conditions. The solutions obtained from each initial condition were separated into two parts, one part is identified as being a transient part and the other as a periodic part. The functional character of the transient part including decay time was dependent on the type of initial condition used while the periodic solution is independent of the initial condition. The two initial conditions that were used are

$$1) \quad \mu_n^1 = 0 \quad (13)$$

$$2) \quad \mu_n^1 = \cos^2[(3/2) \pi(n - 1)\Delta\xi] \quad (14)$$

where

$$n = 1, 2, \dots, N$$

For convenience, equations (13) and (14) will be referred to as conditions (1) and (2), respectively. Condition (1) (eq. (13)) approximates what one would expect in an experiment immediately after the dissociation process for atoms is started. Condition (2) is arbitrary and actually would be difficult to achieve experimentally, but it was used to demonstrate that the desired periodic solution is independent of the initial condition. Physically, this condition is equivalent to distributing atoms between the two planes in such a manner that the atom concentration is dense both at the inlet plane and at a point two-thirds of the way across the test cell from the inlet plane.

The transient that occurs in the transient part of the solution is defined for convenience in the numerical analysis as follows:

$$\epsilon_n^J = \mu_n^{m_s} - \mu_n^{m_J} \quad n = 1, 2, \dots, N \quad (15)$$

where $\mu_n^{m_s}$ is the desired periodic solution at some sufficiently large time indicated by m_s and which is in phase with the solution $\mu_n^{m_J}$, that is,

$$m_s = m_J + \frac{2\pi M}{W \Delta\tau} \quad (16a)$$

where M is an integer and m_J is given by

$$m_J = \frac{2\pi J}{W \Delta\tau} \quad (16b)$$

where J is an integer. Equation (15) defines the transient, but in programming the difference equation, equation (11), for the two initial conditions cited, it was sufficient to let $M = 1$ and $J = 1, 2, \dots$, and then test whether $\epsilon_n^J \sim 0$ to determine transient decay. The quantity ϵ_n^J serves as a measure of the amount the solution differs from the periodic solution measured every period from $\tau = 0$. When ϵ_n^J is zero, then the requirement for a periodic solution is met; that is, $\mu(\xi, \tau) = \mu[\xi, \tau + (2\pi/W)]$. In the numerical work ϵ_n^J was considered negligible when $|\epsilon_n^J| < 10^{-5}$.

The effect of the decay of the transient is observed in the isometric plots given in figure 2. For comparison purposes, the value of the transient ϵ is included for $\xi = 1$ (i.e., $N = 41$) under a few time designations on each figure. Figures 2(a), 2(c), and 2(e) apply to initial conditions specified by equation (13). Figures 2(b), 2(d), and 2(f) apply to conditions specified by equation (14). Figures 2(a) and 2(b) are for the case of zero dissociation frequency, that is, when the atom concentration at the inlet plane is held stationary. Closed-form solutions are obtainable, since there is a steady-state solution in this case, and these provide a means of checking the numerical techniques used. Also since there are fewer events happening, that is, the inlet plane concentration is not varying in time, one can more readily attach significance to the transient part of the solution. In figure 2(a), the transient decay time is defined as the time required for atoms to diffuse into an empty system and continue diffusing until that equilibrium situation is reached wherein the amount of atoms entering the system is balanced by the amount lost by recombination at all points between the two planes. Figure 2(b) illustrates the diffusion and recombination processes that occur when initial condition (2) is used, that is, when a mass of atoms is inserted at the inlet plane and two-thirds of the way from the inlet plane. Here the atoms diffuse in both directions from the two-thirds point while at the same time atoms are diffusing in at the inlet plane. It is observed that for condition (2), the transient is already quite small (-0.063) at $\tau = 0.1$ (see fig. 2(b)), whereas, for condition (1), the transient has only decayed to 0.409 in twice as much time.

Figures 2(c) and 2(d) illustrate the transient part of the solution for the case where the dimensionless frequency at the inlet plane is ten ($W/2\pi = 10$) rather than zero and the dimensionless sink strength is zero ($k_r = 0$), that is, no recombination. It is noted that the time required for the transient to decay when the first condition is applied is more than eight times that required for the second condition.

The situation tends to reverse itself for the higher values of W and k_r as illustrated in figures 2(e) and 2(f) for $W/2\pi = 10$ and $k_r = 10$. One observes that the decay time for initial condition (1) is about one-half the time required in figure 2(c), but the time required for condition (2) (see fig. 2(f)) is increased by a factor of more than three. An increased time is required for the atoms to recombine and thus decrease their number to that required for the periodic variation. From these results, it would be anticipated that for values of k_r greater than about 15, the initial condition specified by equation (13) yields the faster transient decay time. For sink strength values less than 15, the transient decay is faster when the initial condition is given by equation (14).

The two initial conditions specified could no doubt be improved upon in order to arrive more quickly at the periodic solution. In any event, the better initial conditions would depend on W and k_r including, of course, the exact initial condition which is known only after the problem is solved.

Solution - Periodic Part

The proposed experiment that prompted the analysis contained in this report utilizes measurements made on the variation in concentration to determine the diffusion and recombination rates and for this reason it is of interest to view curves illustrating this variation, that is, curves illustrating the upper and lower bounds within which the concentration varies. The curves for varying sink strengths illustrated in figure 3 are projections of the concentration curves at various instants of time on the (μ, ξ) plane after the transient has decayed and the periodic solution is dominant. These projections were obtained by plotting the values of the periodically varying concentration at twenty equidistant points in dimensionless time, in one period, using an automatic plotter. The resulting system of curves then define a set of upper and lower envelopes within which the concentration varies. The envelopes are dependent only on the values of the dimensionless parameter frequency W and sink strength k_r . One observes in figure 3 that for increasing sink strength the mean values of the concentration variation become smaller, that is, the envelopes shift to lower values of concentration. This follows as a result of the greater loss of atoms due to the increasingly greater rate of recombination. One also observes that there is a decrease in the difference between the upper and lower envelopes; that is, there is a decrease in the amplitude of the variation in concentration that is due both to dimensionless frequency and sink strength. The functional dependence of the difference between the upper and lower envelopes on sink strength and frequency can be determined by defining a parameter ξ_E , called the penetration depth, and then determining the dependence of this parameter on W and k_r . The penetration depth is defined as the distance from the inlet plane at which the amplitude of

the variation in the concentration has decreased to some specified value, say E , compared to its value at the inlet plane. The value E will be called the decay fraction and is given by

$$E = \frac{\mu_{\max}(\xi_E) - \mu_{\min}(\xi_E)}{\mu_{\max}(0) - \mu_{\min}(0)} \quad (17)$$

where $\mu_{\max}(\xi)$ and $\mu_{\min}(\xi)$ are the values of the upper and the lower envelopes defining the variation in concentration illustrated in figure 3. The equations are normalized such that

$$\mu_{\max}(0) - \mu_{\min}(0) = 1 \quad (18)$$

The problem now is to determine the explicit dependence of ξ_E on the parameters W and k_r by solving the implicit expression given by

$$E = \mu_{\max}(\xi_E) - \mu_{\min}(\xi_E) \quad (19)$$

The solution of equation (19) is obtained by measuring the difference between the upper and lower envelopes that are obtained from the periodic part of the solution and finding that point where the difference is E . The corresponding value of ξ obtained is the penetration depth ξ_E . The results from these measurements are plotted in figures 4(a) and 4(b) where E is arbitrarily chosen as $1/e$ and $1/4$, respectively. These figures are plots of penetration depth ξ_E versus dimensionless frequency $W/2\pi$ for various values of the dimensionless sink strength. The features common to both these figures and therefore independent of the value of E are described as follows: One observes that for high frequencies the decrease in concentration variation occurs close to the inlet plane and is little affected by the sink strength k_r . For example, when the dimensionless frequency $W/2\pi$ is of order 20 or greater, the variation decrease characterized by ξ_E occurs within about $1/10$ of the diffusion tube length and depends very little on the value of the sink term parameter k_r . As the frequency is reduced, there is a greater dependence of the depth parameter ξ_E on sink strength, and the decay occurs farther from the inlet. Also in both figures, one observes that when sink strength is large the decay occurs near the inlet plane and is little affected by frequency. From the preceding discussion it is noted that the greatest spread in the penetration depth with respect to sink strength is obtained at low frequencies.

DISCUSSION

In the section that follows the major errors that occur in the numerical calculation will be analyzed. In the second section that follows a few remarks

will be made on the comparison of the closed-form solution given in reference 1, that was obtained from a linearized sink term, with the results obtained from the numerical solution discussed in this report with a nonlinear sink term. The third section will include a few remarks on the application of the penetration depth to experimentally determine the diffusion and recombination rates.

Numerical Errors

The electronic computer cycles through the numerical equations a considerable number of times before obtaining the periodic solution. For example, when $N = 41$, the computer cycled through the numerical equations 1922 times just to increase the dimensionless time from $\tau = 0$ to $\tau = 0.22$ and obtain the data for figure 2(a). Such a large number of calculations may reduce the accuracy of the numbers because of accumulated round-off errors. Also, since a solution is being obtained for a set of difference equations which depend on grid spacings, there is the further possibility that the final answers may be in error because of the large grid spacings.

It was possible to investigate the errors arising in the numerical calculations by using as a comparison two independent closed-form solutions which are obtainable from degenerate forms of equations (4). The first degenerate form results from setting zero forcing frequency as the boundary condition at the inlet plane to obtain $\mu(0) = 1.0$ (see eq. (4b)), and setting the dimensionless time derivative in equation (4a) equal to zero. The resulting time independent solution is an elliptic integral expressing the dimensionless concentration $\mu(\xi)$ implicitly in terms of the dimensionless distance ξ (see appendix); that is,

$$\xi = 1 - \frac{3^{1/4}}{\sqrt{2k_T\mu(1)}} F\left\{\varphi[\mu(\xi);\mu(1)], C\right\} \quad (20)$$

where

$$\varphi[\mu(\xi);\mu(1)] = \cos^{-1} \left[\frac{\mu(1)(\sqrt{3} + 1) - \mu(\xi)}{\mu(1)(\sqrt{3} - 1) + \mu(\xi)} \right] \quad (20a)$$

and

$$C = \frac{1}{2} \sqrt{2 - \sqrt{3}} \quad (20b)$$

The function $F(\varphi, C)$ is the incomplete elliptic integral of the first kind with argument φ and modulus C , and $\mu(1)$ is the value of the concentration at the far boundary determined by solving equation (20) for $\mu(1)$ when $\xi = 0$. The solution $\mu(\xi)$ corresponds to the steady-state solution of $\mu(\xi, \tau)$ obtained after transient decay for cases of the type shown in figures 2(a) and 2(b).

The second degenerate form for which a closed-form solution is available is the case wherein the sink strength is set equal to zero. Here the solution of equation (4a), obtained in the limit when $k_r = 0$, is given by equation (105) in reference 1. For the concentration normalized so that the maximum value of $\mu(\xi, \tau)$ is 1, we obtain

$$\mu(\xi, \tau) = \frac{1}{2} + \text{Real} \left\{ e^{iW\tau} \frac{\cosh[\sqrt{W/2} (1+i)(\xi-1)]}{2 \cosh[\sqrt{W/2} (1+i)]} \right\} \quad (21)$$

Equation (21) corresponds to the periodic solution $\mu(\xi, \tau)$ obtained after the transient decay for cases of the type illustrated in figures 2(c) and 2(d).

The errors in the numerically determined steady-state solution, that is, the numerical solution minus equation (20) all divided by equation (20), are shown as a function of mesh size $\Delta\xi$ in figure 5. This figure illustrates the errors just for one example where the sink strength was arbitrarily chosen equal to 10. The upper curve gives the percent error of the far boundary value of the dimensionless concentration and the lower curve gives the percent error in the concentration midway between the boundary planes. The worst error due to a mesh occurs at the far boundary plane and is about 3 percent for $\Delta\xi = 0.05$ or $N = 21$ (see eq. (5a)). The error in the dimensionless concentration at points closer to the inlet boundary plane is less, and at the midpoint the error is 0.7 percent for the same mesh size. It is interesting to observe that for both values, the error does not change in sign and appears to be linearly decreasing with smaller mesh size.

The error in values of the concentration at the far boundary plane as a function of sink strength is shown in figure 6 for specific mesh sizes $\Delta\xi = 0.025$ and 0.04 ($N = 41$ and 26 , respectively). In this figure the errors in the numerical solution are also related to values of the concentration determined from equation (20). One observes a greater dependence of error on sink strength for large mesh sizes than for small sizes. This is indicated by the increase in error from 2.4 percent at $k_r = 10$ to 3.7 percent at $k_r = 70$ (an increase of 1.3 percent) while the corresponding increase for $\Delta\xi = 0.025$ is from 1.4 to 2.2 percent (an increase of 0.8 percent). One also observes an abrupt decrease in the error for values of the sink strength less than 5 and the error is negligible in the numerical calculation for the case of zero sink strength.

When equation (21) is used as the basis of comparison it is possible to obtain a check of the error in the numerically determined penetration depth, but only for zero sink strength. It is found that when the mesh size is greater than 0.067 ($N = 16$), the error in the penetration depth is small, only 0.01 percent, and depends very little on mesh size. This observation is consistent with the findings illustrated in figure 6 where it was found that the error was negligible for zero sink strength. This small error may be due to causes other than mesh size. It is about the order of magnitude expected of round-off errors and of errors due to inaccuracies in the various subroutines used in programming the numerical equations for the electronic computer. With interval spacings greater

than 0.067 the error in penetration depth is large and erratic in nature. This may be due to the fact that the corresponding large mesh size that results for the time variable $\Delta\tau$ (see eq. (10a)) makes a numerical differentiation of the concentration curves inaccurate; therefore the upper and lower envelopes defining the concentration variation are in error. This would then cause a large and erratic error in the determination of the penetration depth.

It is not possible, with the available closed-form solutions, to check the error of the penetration depth for sink strength values other than zero. It is expected, however, that any numerical errors that do occur would be less than the worst error that is found for the far boundary value of the concentration shown in figure 6, for two reasons: First, all mesh size errors are of one sign and therefore should be partially subtracted (see eq. (19)); second, the penetration depth corresponds to values of the concentration closer to the inlet plane where error is less than the far boundary value of error (see fig. 5).

The Linear Sink Term as an Approximation to the Nonlinear Sink Term

Since the first solution obtained (see ref. 1) is a closed-form solution for a linearized sink term, it is of interest to compare the linear solution obtained in reference 1 with the numerical solution for the nonlinear sink term. The nonlinear sink term given by equation (66a) in reference 1 is

$$k_N(\mu) = -k_R\mu_1^2 \quad (22)$$

The linear sink term is given by

$$k_L(\mu) = -k_R'\mu_1 = -k_R\bar{\mu}\mu_1 \quad (23)$$

where the subscripts N and L are used here to differentiate between nonlinear and linear, respectively, and $\bar{\mu}$ is a constant which represents the average value of the solution for the nonlinear sink term. The expression from which the depth parameter can be obtained in the linear problem (see eq. (106), ref. 1) is given by

$$\frac{\cosh[P_1(\xi_E - 1)]}{\cosh p_1} = E \quad (24)$$

where

$$P_1 = \sqrt{\frac{k_R'}{2}} \left[\sqrt{\sqrt{1 + \left(\frac{W}{k_R'}\right)^2} + 1} + i \sqrt{\sqrt{1 + \left(\frac{W}{k_R'}\right)^2} - 1} \right]$$

The penetration depth curves obtained from equation (24) are compared with those obtained numerically in figure 7. The decay fraction E is $1/e$. From equation (23) with $\bar{\mu} = 1/2$ one observes that the linear sink term curves for $k_r^1 = 10$ and 20 are approximations for the nonlinear sink term curves $k_r = 20$ and 40, respectively. The curves shown in figure 7 for these corresponding values of k_r and k_r^1 indicate that the linear approximation $\bar{\mu} = 1/2$ is not good, but one does note that the results could be made to agree better by taking a different value for $\bar{\mu}$. This follows if one notes that a curve for $k_r^1 = 15$ would be a good approximation for $k_r = 20$ except at low frequencies. One also observes that the results agree better for higher frequencies. This follows since as the frequency increases, the effect of the sink term on the penetration depth decreases.

Experimental Application of the Penetration Depth Results

Inasmuch as the analysis contained in this report was prompted by a proposed experiment, a few remarks will be made on the application of the results to the determination of diffusion and recombination rates.

The solutions giving penetration depth versus frequency with the sink strength as a parameter can be used in conjunction with experimentally determined values of penetration depth where the frequency, degree of dissociation, and partial number densities would be controlled, to obtain appropriate values for the sink strength and diffusion coefficients. It may be necessary to make a judicious choice for the inert gas that would be used in the system in order that D_{23} (and perhaps also D_{13}) would be known or to make certain assumptions regarding the equality of the intermolecular potentials in order to decrease the number of unknowns. This decision should depend in part on the uncertainty in measured values due to experimental errors. Also, wall reactions were neglected in the equations used in this report and therefore in an experiment consideration will have to be given to minimizing loss of atoms due to wall recombination. If the walls of a test cell are constructed of pyrex and if the pressure is not too low it is expected that the loss of atoms due to the wall reaction will be small compared to the losses due to homogeneous recombination. In this respect any effects due to the wall may possibly be handled by introduction of a correction term in the differential equation.

The results obtained for the penetration depth as a function of frequency and sink strength given in this report apply only to the atoms in the ternary mixture of atoms, molecules, and an inert gas. The experiment outlined in reference 1 makes use of vacuum ultraviolet absorption measurements on oxygen molecules; therefore the results obtained numerically may not be directly applicable. Direct use of the calculations requires that a narrow line source of radiation for atomic absorption be available if similar absorption techniques are to be applied to the atomic oxygen in the system. Comparable solutions are obtainable for oxygen molecules by a minor extension of the techniques used in this report. This extension is described in reference 1.

CONCLUDING REMARKS

A numerical method has been developed to determine the periodic solution of a unidimensional time varying diffusion equation with a nonlinear sink term and unsteady boundary conditions. An initial condition that is not specifically known is required in the numerical procedure. It is shown that any arbitrary choice of initial condition merely results in a transient effect that decays as the time variable increases in value. The solution that remains is periodic and independent of the initial condition. For a given initial condition the transient decay time is dependent both on the frequency of the concentration variation and on the sink strength.

The periodic solution is used to obtain values of the penetration depth which is the depth at which the amplitude of the concentration variation has decreased to some specified fraction of its inlet value. The solutions giving penetration depth versus frequency with the sink strength as a parameter can be used in conjunction with experimentally determined values of penetration depth to obtain appropriate values of the sink strength and diffusion coefficients. In order to obtain maximum resolution in the determination of the desired rates it is necessary that the concentration variation frequency be low.

The errors that result from the numerical techniques used in obtaining the periodic solution can be controlled by proper choice of mesh size. These errors are negligible in the results given for the penetration depth.

The system of equations that were solved in this report are in a general form, and, although continual reference was made to a diffusion experiment, the results are not so restricted. The solutions are applicable to any diffusion or any physical problem that can be described as a diffusion equation with a sink term. The numerical method that was used is not restricted by the sign of the sink (source) term and the method may also be extended to include any degree of nonlinearity in the sink term.

Ames Research Center
National Aeronautics and Space Administration
Moffett Field, Calif., Oct. 23, 1963

APPENDIX A

DERIVATION OF EQUATION (20)

In the text, equation (20) was given without a description of the methods leading to its derivation. Equation (20) relates implicitly the dimensionless concentration of atoms $\mu(\xi)$ in terms of the coordinate ξ for the steady-state problem that describes diffusion with recombination in the region between two planes, the inlet and far boundary planes. The problem applies to the physical situation that exists when the atoms lost by recombination are balanced by the atoms gained by diffusion at each station between the two planes. In order to keep the inlet plane concentration, $\mu(0) = 1$, a constant, fresh atoms must be continually added at the inlet plane to replenish those that are lost. Chemical reaction of the atoms with the far boundary plane is assumed to be negligible. The basic differential equation that describes this problem is obtained by setting the time derivative $\partial\mu/\partial\tau$ in equation (4a) equal to zero to obtain the nonlinear ordinary differential equation given by

$$\frac{d^2\mu}{d\xi^2} = k_r\mu^2 \quad (A1)$$

The boundary conditions are given by equations (4b) and (4c) where the dissociation frequency W in equation (4b) is set equal to zero, that is,

$$\mu(0) = 1 \quad (A2)$$

$$\left. \frac{\partial\mu}{\partial\xi} \right|_{\xi=1} = 0 \quad (A3)$$

Since the problem excludes time dependence an expression for the initial condition is, of course, not required.

The solution is obtained by first multiplying both sides of equation (A1) by $d\mu/d\xi$ to obtain

$$\frac{d}{d\xi} \left[\frac{1}{2} \left(\frac{d\mu}{d\xi} \right)^2 \right] = \frac{k_r}{3} \frac{d(\mu^3)}{d\xi} \quad (A4)$$

Equation (A4) is integrated and the constant of integration then determined using equation (A3). The resulting expression is solved for $\frac{d[\mu(\xi)/\mu(1)]}{d\xi}$ to obtain

$$\frac{d}{d\xi} \left[\frac{\mu(\xi)}{\mu(1)} \right] = -\sqrt{\frac{2}{3} k_r \mu(1)} \left\{ \left[\frac{\mu(\xi)}{\mu(1)} \right]^3 - 1 \right\}^{1/2} \quad (A5)$$

where $\mu(1)$ is the value of the dimensionless concentration at the far boundary. The negative sign of the square root is required because the concentration is always decreasing. The integral form for equation (A5) is given by

$$\xi = 1 - \frac{1}{\sqrt{(2/3)k_r\mu(1)}} \int_1^{t_1} \frac{dt}{\sqrt{t^3 - 1}} \quad (A6)$$

where

$$t_1 = \mu(\xi)/\mu(1) \quad (A6a)$$

The integral in equation (A6) is proportional to the incomplete elliptic integral of the first kind (see ref. 3); that is,

$$\int_1^{t_1} \frac{dt}{\sqrt{t^3 - 1}} = 3^{-1/4} F(\varphi, C) \quad (A7)$$

where the argument and modulus are given, respectively, by

$$\varphi = \cos^{-1} \left(\frac{\sqrt{3} + 1 - t_1}{\sqrt{3} - 1 + t_1} \right) \quad (A7a)$$

$$C = \frac{1}{2} \sqrt{2 - \sqrt{3}} \quad (A7b)$$

Substitution of equation (A7) into equation (A6) yields

$$\xi = 1 - \frac{3^{1/4}}{\sqrt{2k_r\mu(1)}} F \left\{ \varphi[\mu(\xi); \mu(1)], C \right\} \quad (A8)$$

where

$$\varphi \left[\mu(\xi); \mu(1) \right] = \cos^{-1} \left[\frac{\mu(1)(\sqrt{3} + 1) - \mu(\xi)}{\mu(1)(\sqrt{3} - 1) + \mu(\xi)} \right] \quad (A8a)$$

The value of $\mu(1)$ is determined from the implicit expression obtained by first letting $\xi = 0$ in equation (A8) and then substituting the boundary condition given by equation (A2) for $\mu(0)$ to obtain

$$F \left\{ \phi[1; \mu(1)], C \right\} = \frac{\sqrt{2k_r \mu(1)}}{3^{1/4}} \quad (A9)$$

The constant $\mu(1)$ is dependent only on the value of the sink strength k_r . Once $\mu(1)$ is determined, equation (A8) can be solved to determine $\mu(\xi)$.

REFERENCES

1. Reinhardt, Walter A.: Theoretical Investigation of Unsteady Diffusion With Recombination in a Ternary Mixture of Diatomic Molecules, Dissociated Atoms, and an Inert Gas. NASA TN D-1651, 1963.
2. Richtmyer, Robert D.: Difference Methods for Initial-Value Problems. Ch. 1, Interscience Pub., Inc., N. Y., 1957.
3. Byrd, Paul F., and Friedman, Morris D.: Handbook of Elliptic Integrals for Engineers and Physicists. Springer-Verlag, Berlin-Gottingen-Heidelberg, 1954, p. 87.

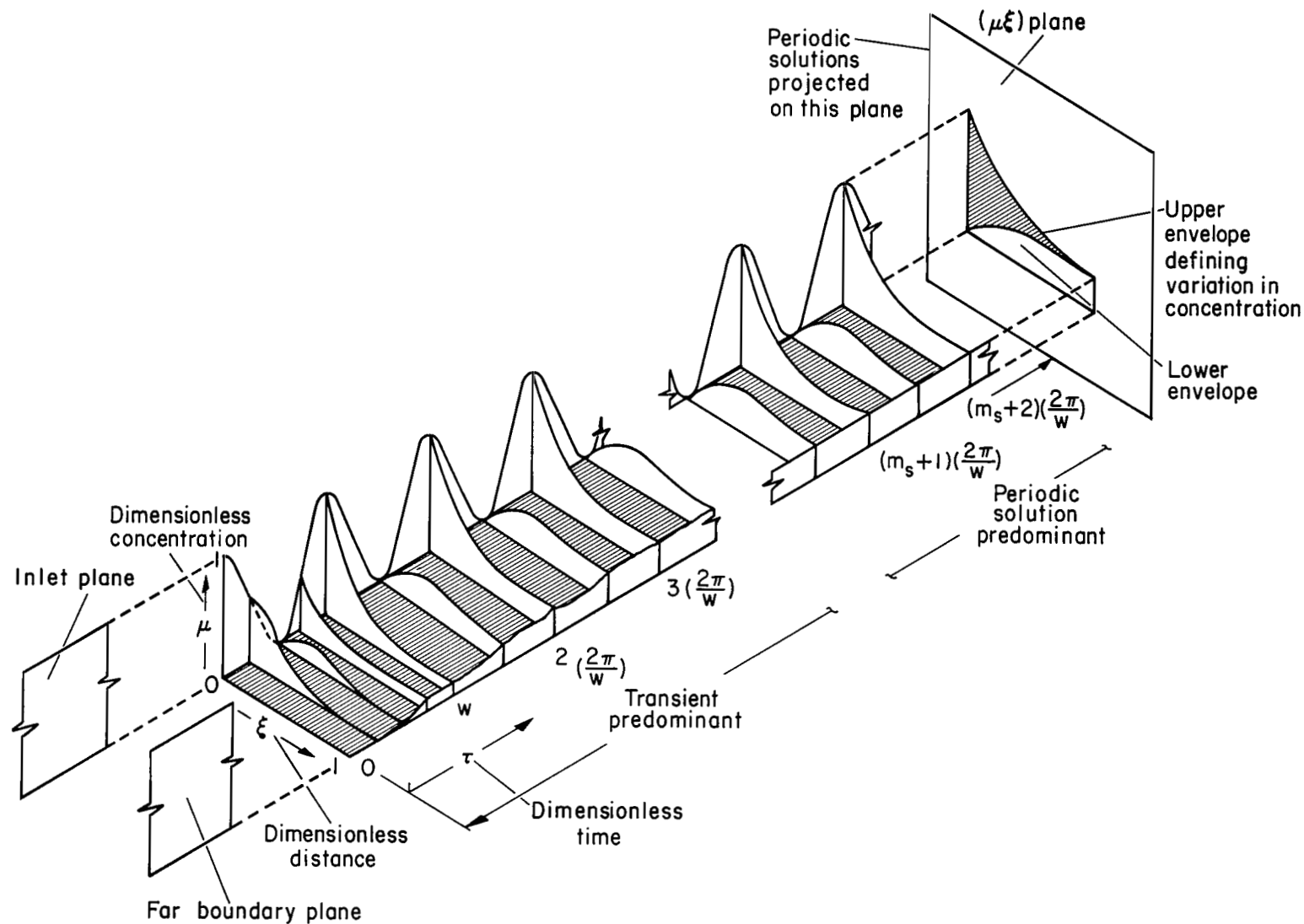
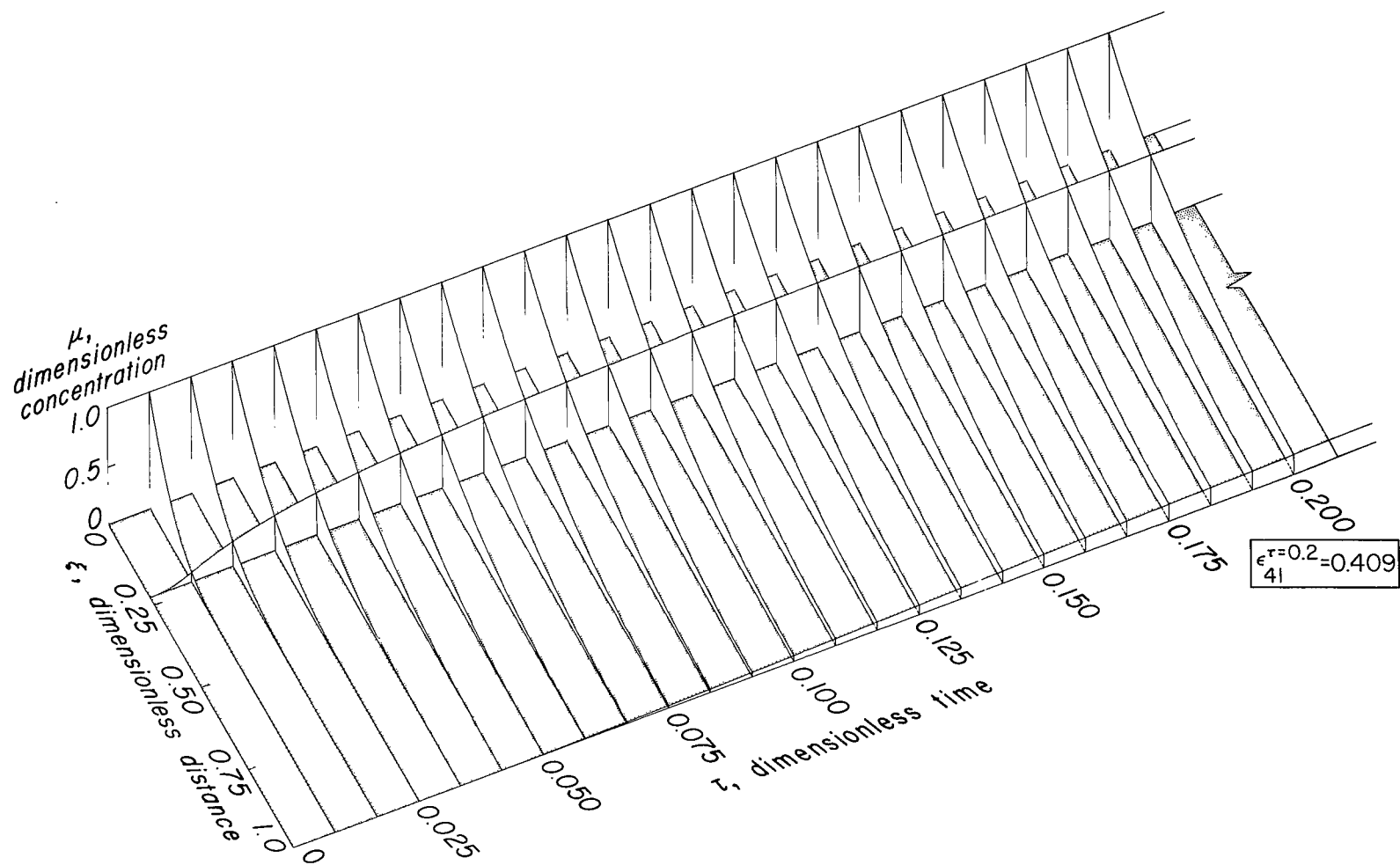
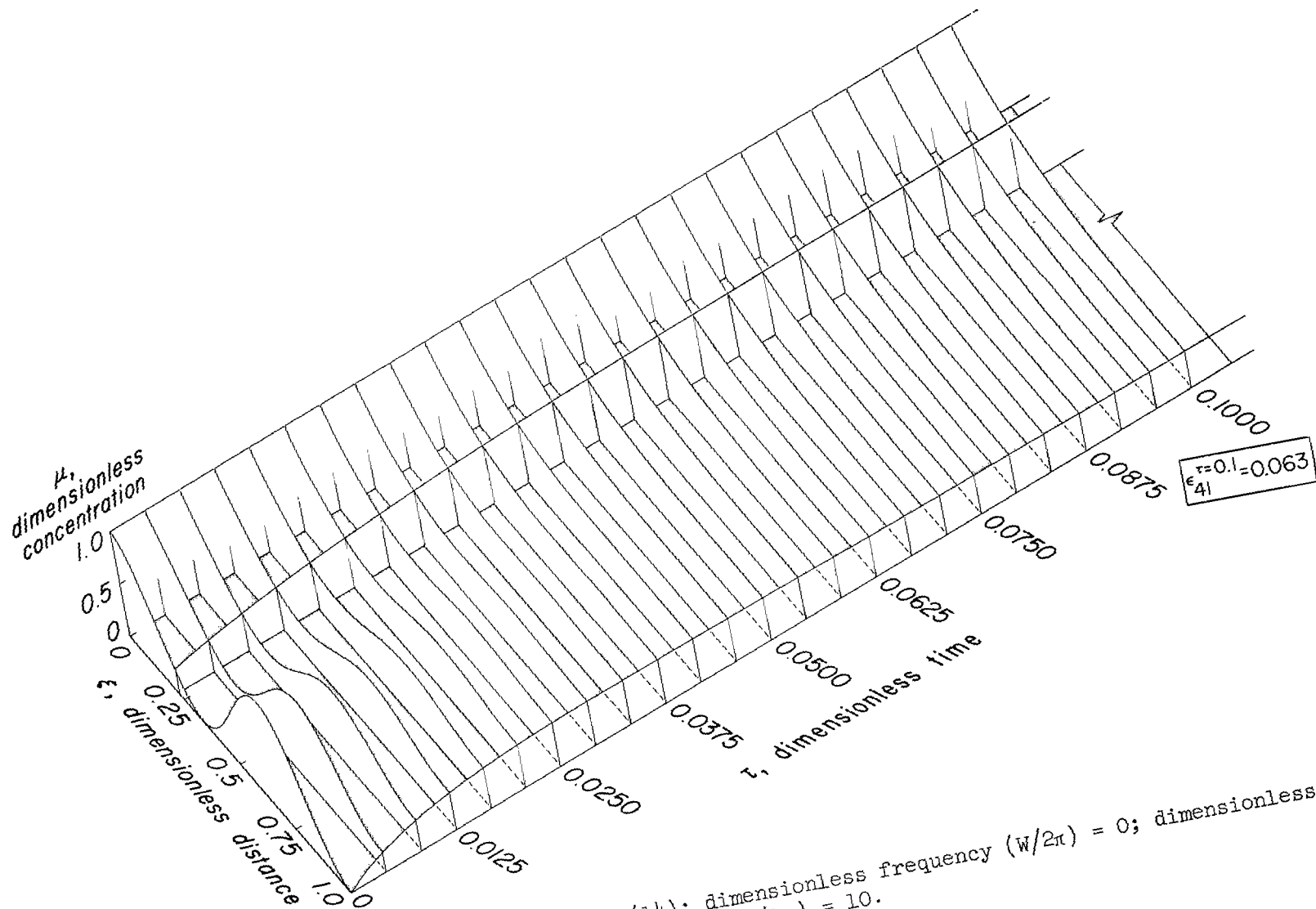


Figure 1.- Sketch illustrating the pertinent features of the solution $\mu(\xi, \tau)$.

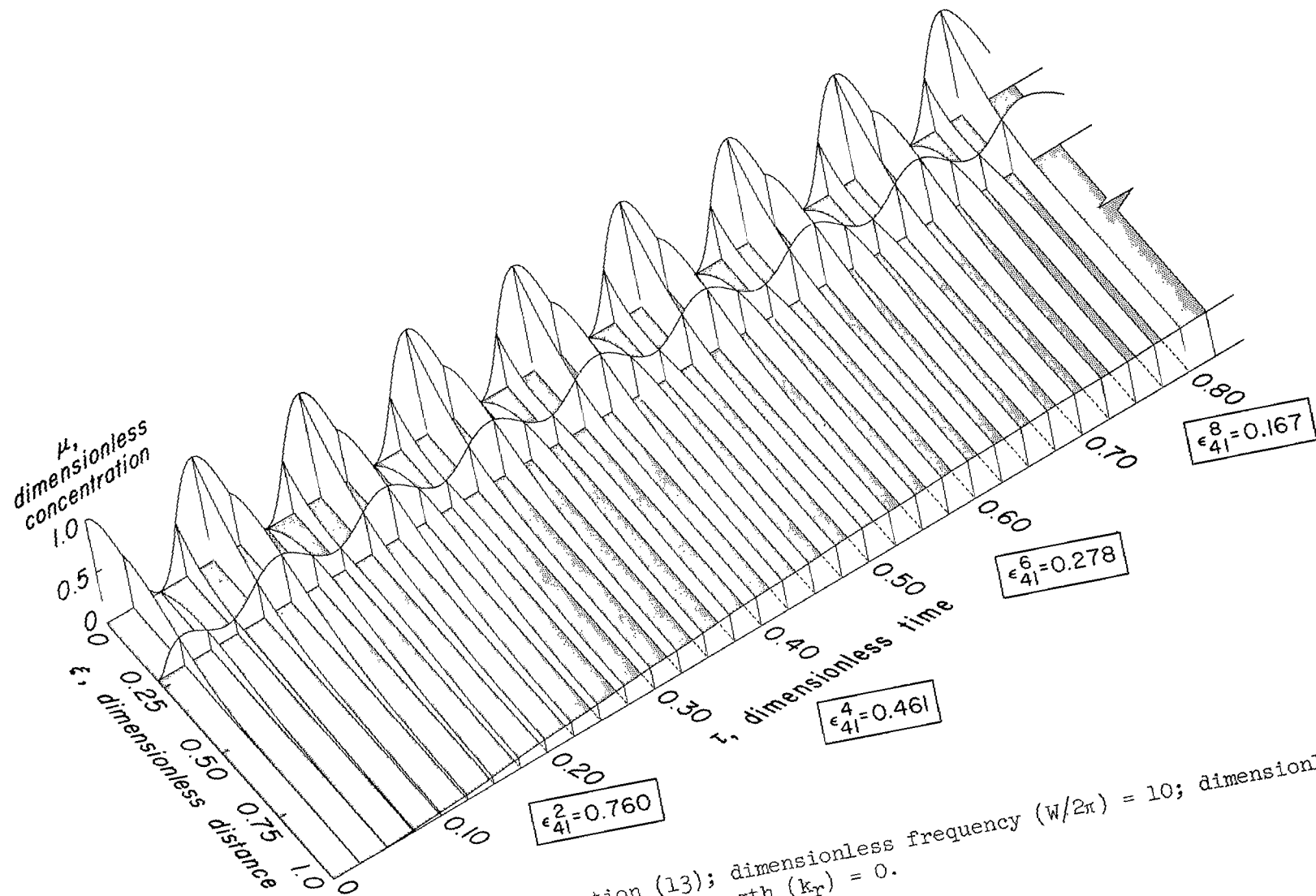


(a) Initial condition given by equation (13); dimensionless frequency ($W/2\pi$) = 0; dimensionless sink strength (k_r) = 10.

Figure 2.- Isometric plots of dimensionless concentration $\mu(\xi, \tau)$ showing transient decay for two different initial conditions and given values of dimensionless frequency ($W/2\pi$) and dimensionless sink strength (k_r).

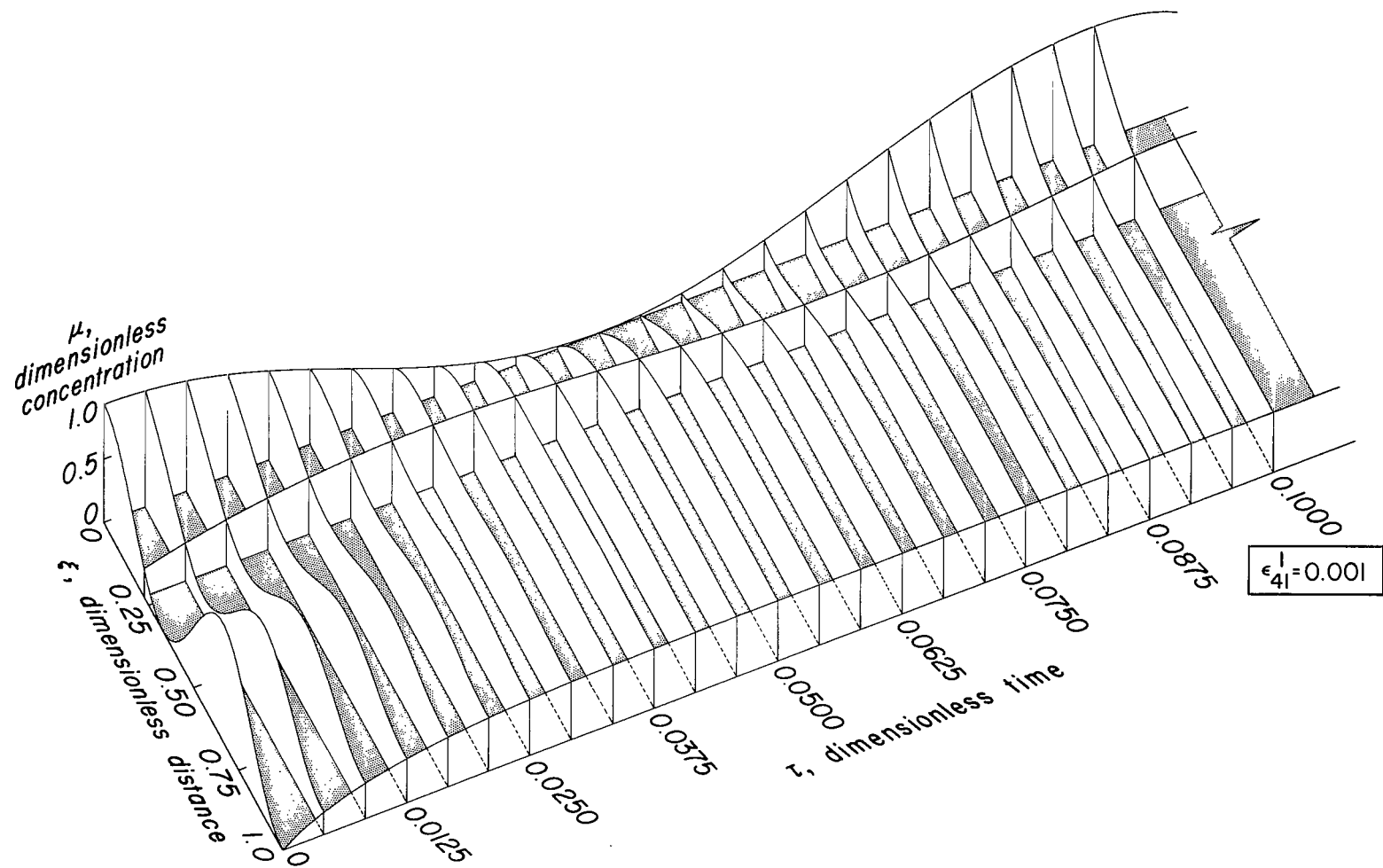


(b) Initial condition given by equation (14); dimensionless frequency $(w/2\pi) = 0$; dimensionless sink strength $(k_r) = 10$.
 Figure 2.- Continued.



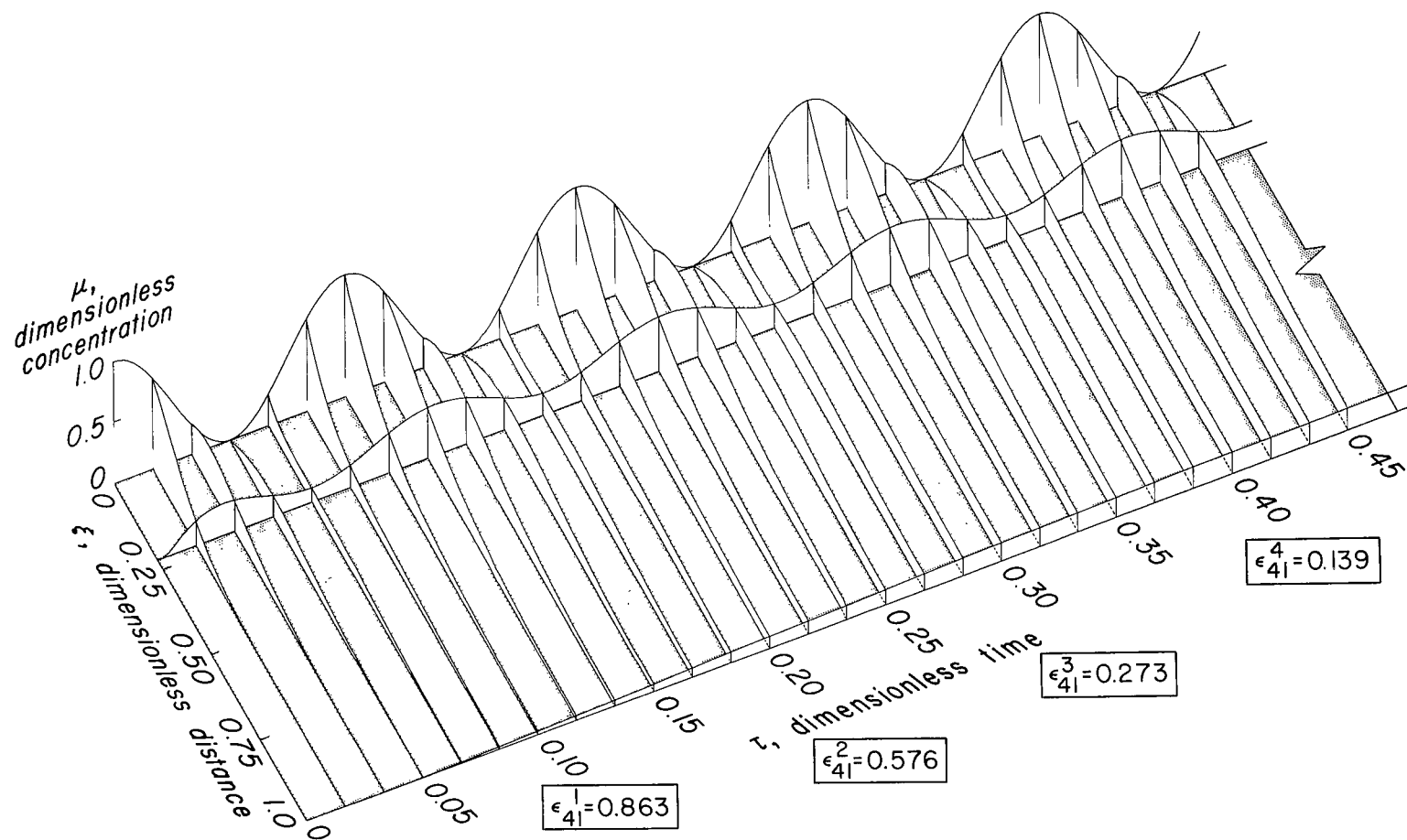
(c) Initial condition given by equation (13); dimensionless frequency $(W/2\pi) = 10$; dimensionless sink strength $(k_r) = 0$.

Figure 2.- Continued.



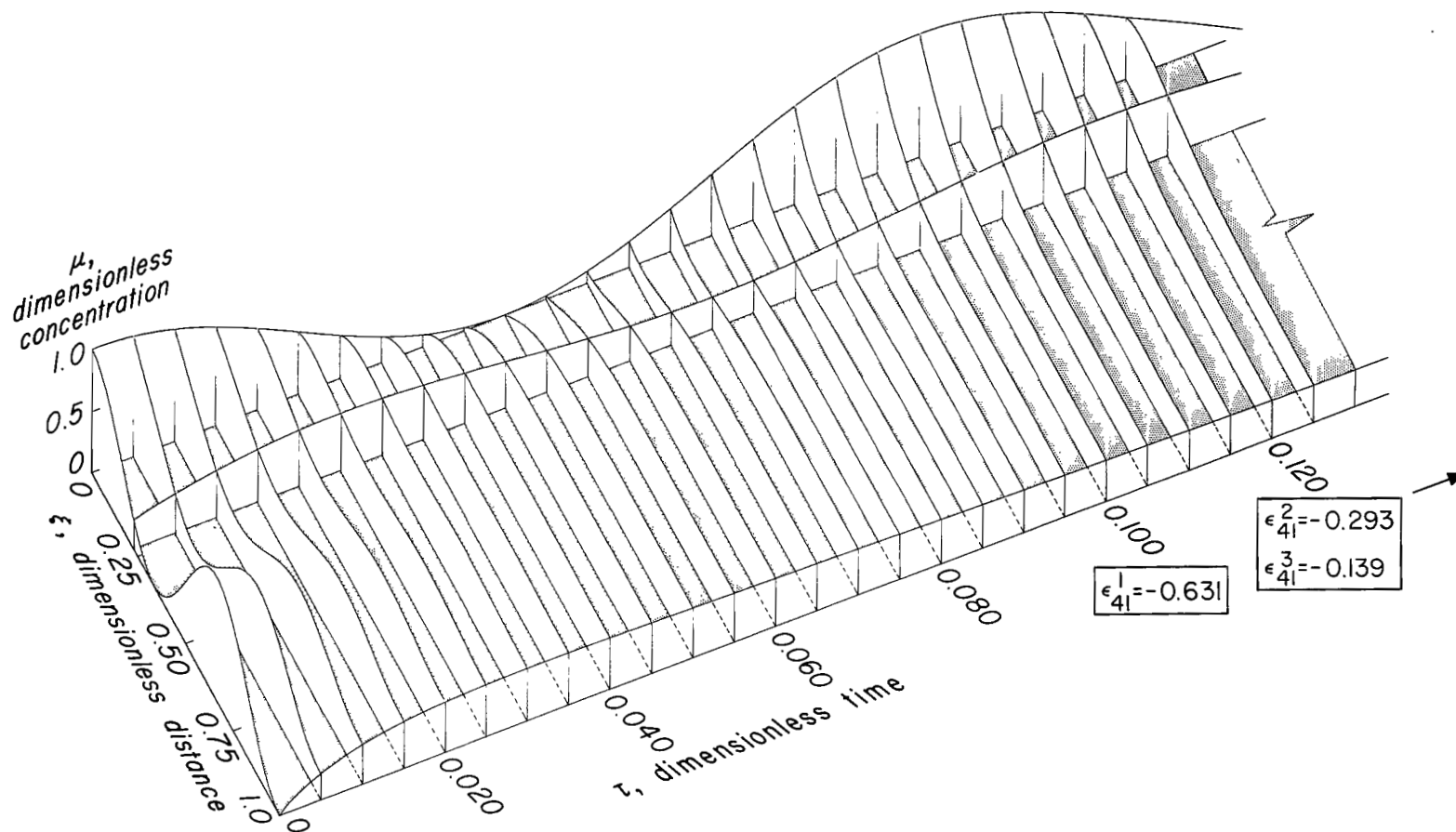
(d) Initial condition given by equation (14); dimensionless frequency ($w/2\pi$) = 10; dimensionless sink strength (k_r) = 0.

Figure 2.- Continued.



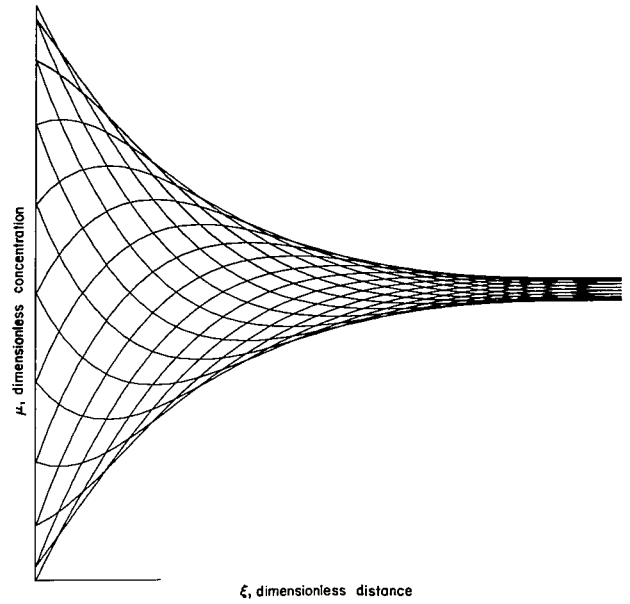
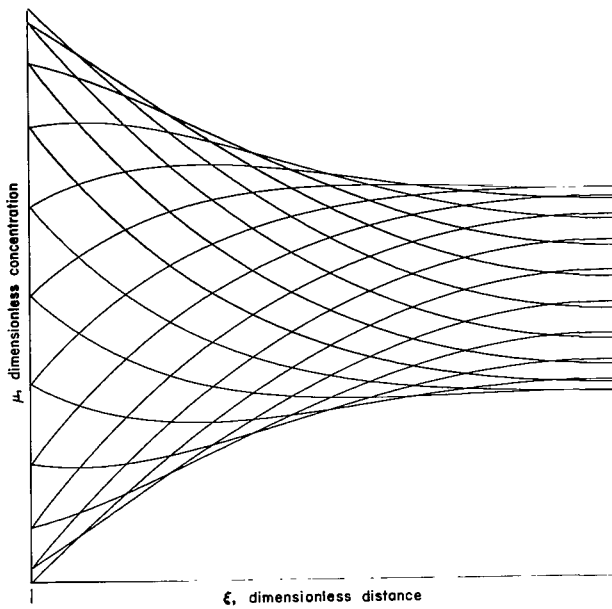
(e) Initial condition given by equation (13); dimensionless frequency ($W/2\pi$) = 10; dimensionless sink strength (k_r) = 10.

Figure 2.- Continued.

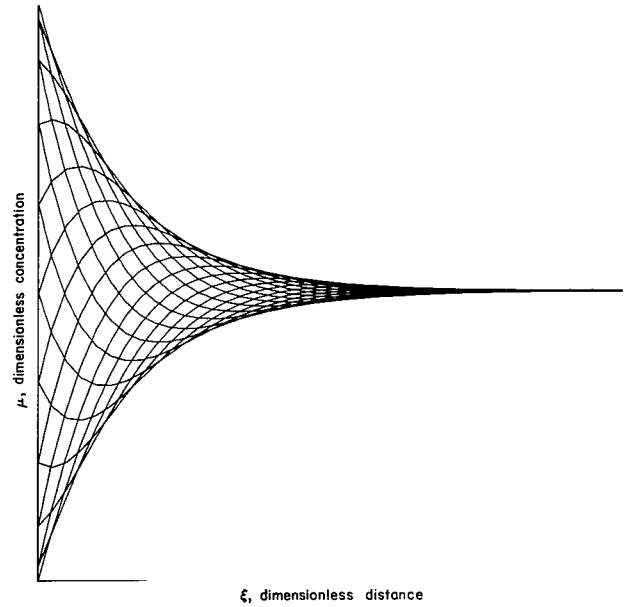
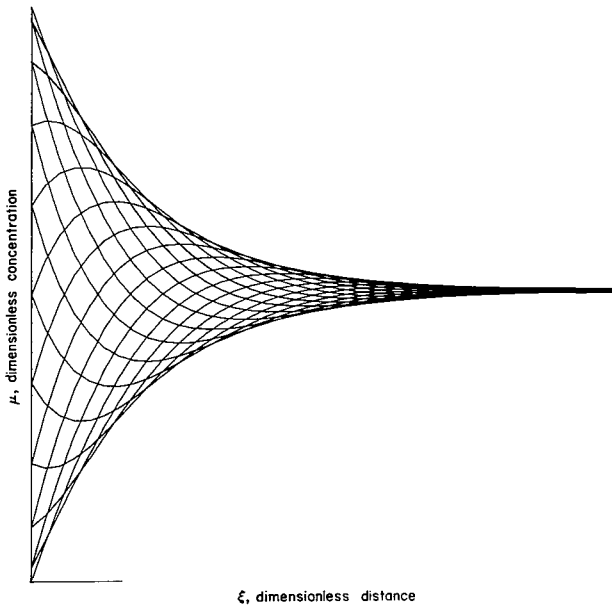


(f) Initial condition given by equation (14); dimensionless frequency ($W/2\pi$) = 10; dimensionless sink strength (k_r) = 10.

Figure 2.- Concluded.

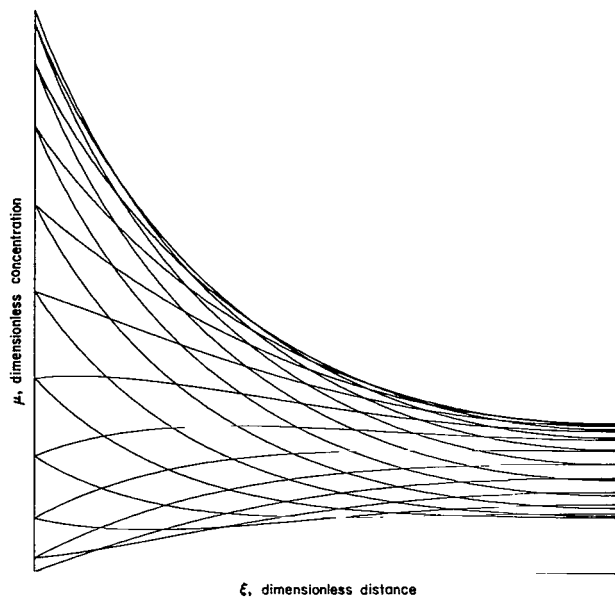


(a) Dimensionless sink strength (k_r) = 0; (b) Dimensionless sink strength (k_r) = 0;
dimensionless frequency ($W/2\pi$) = 1. dimensionless frequency ($W/2\pi$) = 5.

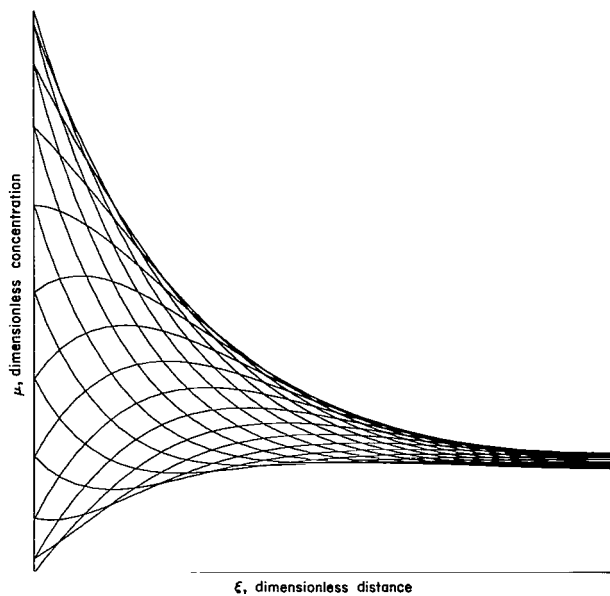


(c) Dimensionless sink strength (k_r) = 0; (d) Dimensionless sink strength (k_r) = 0;
dimensionless frequency ($W/2\pi$) = 10. dimensionless frequency ($W/2\pi$) = 15.

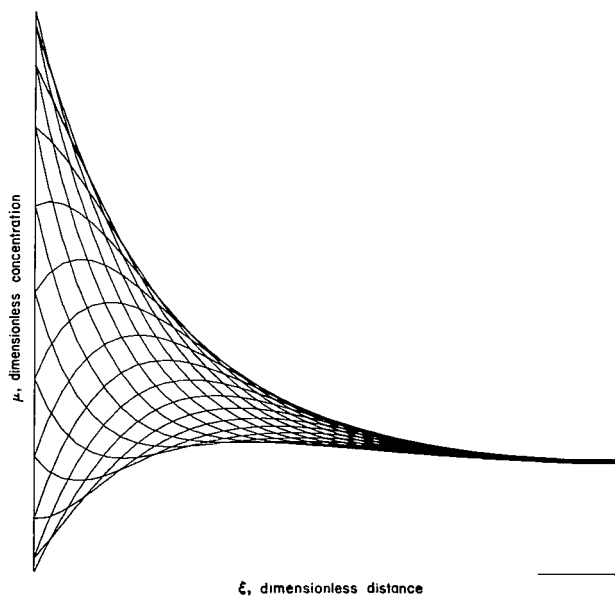
Figure 3.- Steady-state concentration variation curves for various values of the dimensionless frequency and sink strength.



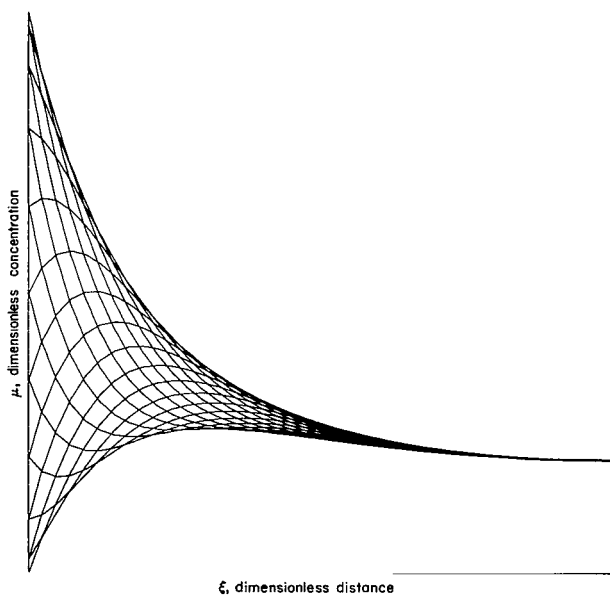
(e) Dimensionless sink strength (k_r) = 10; dimensionless frequency ($W/2\pi$) = 1.



(f) Dimensionless sink strength (k_r) = 10; dimensionless frequency ($W/2\pi$) = 5.

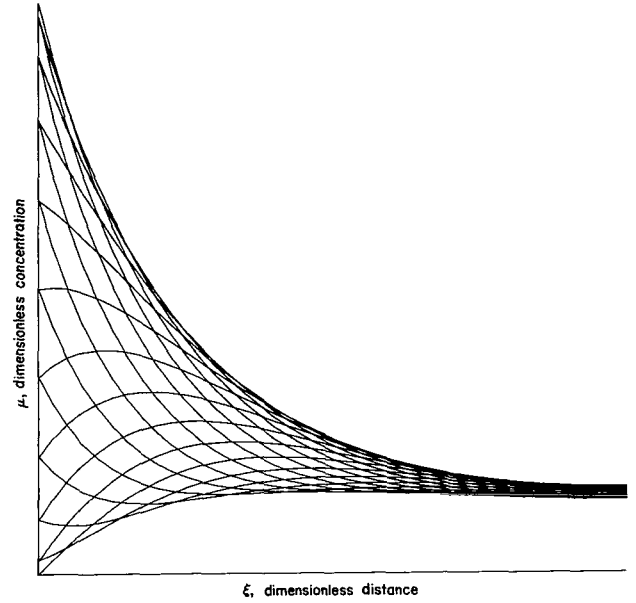
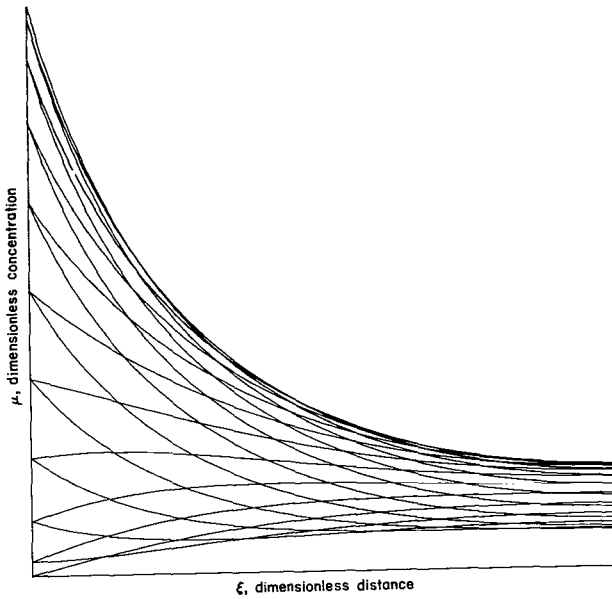


(g) Dimensionless sink strength (k_r) = 10; dimensionless frequency ($W/2\pi$) = 10.

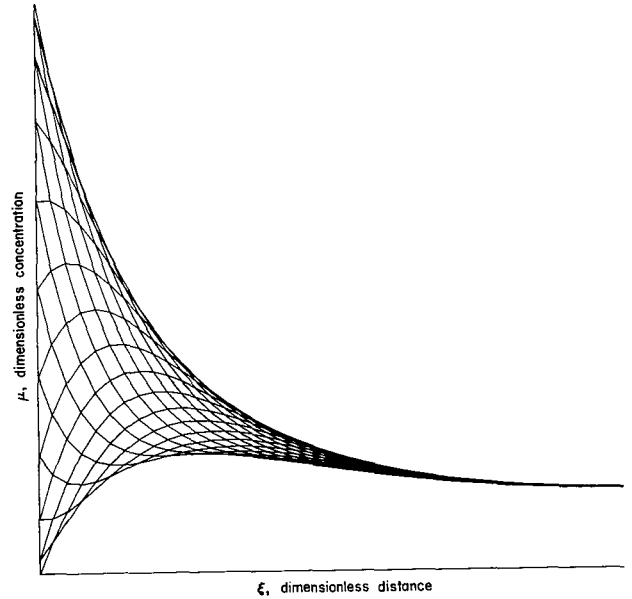
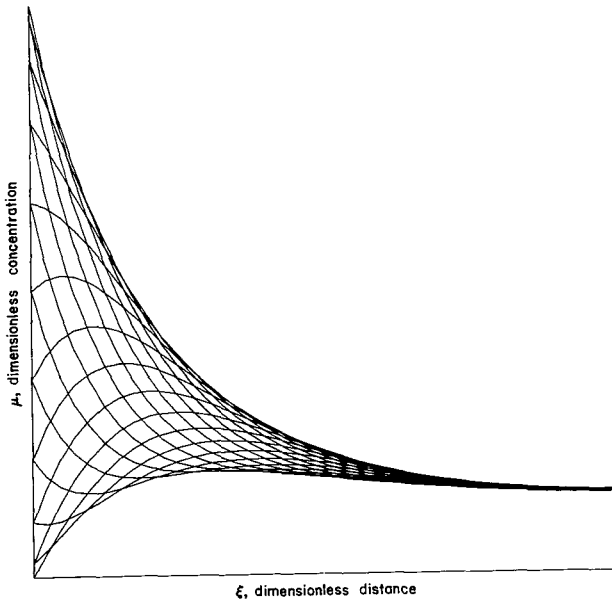


(h) Dimensionless sink strength (k_r) = 10; dimensionless frequency ($W/2\pi$) = 15.

Figure 3.- Continued.

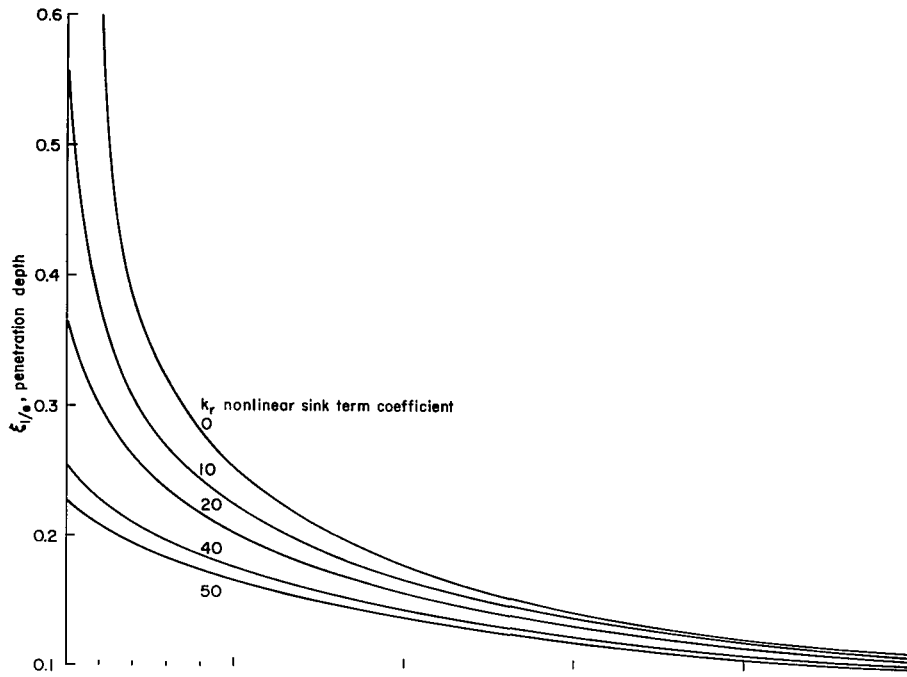


- (i) Dimensionless sink strength (k_r) = 20; (j) Dimensionless sink strength (k_r) = 20;
dimensionless frequency ($W/2\pi$) = 1. dimensionless frequency ($W/2\pi$) = 5.

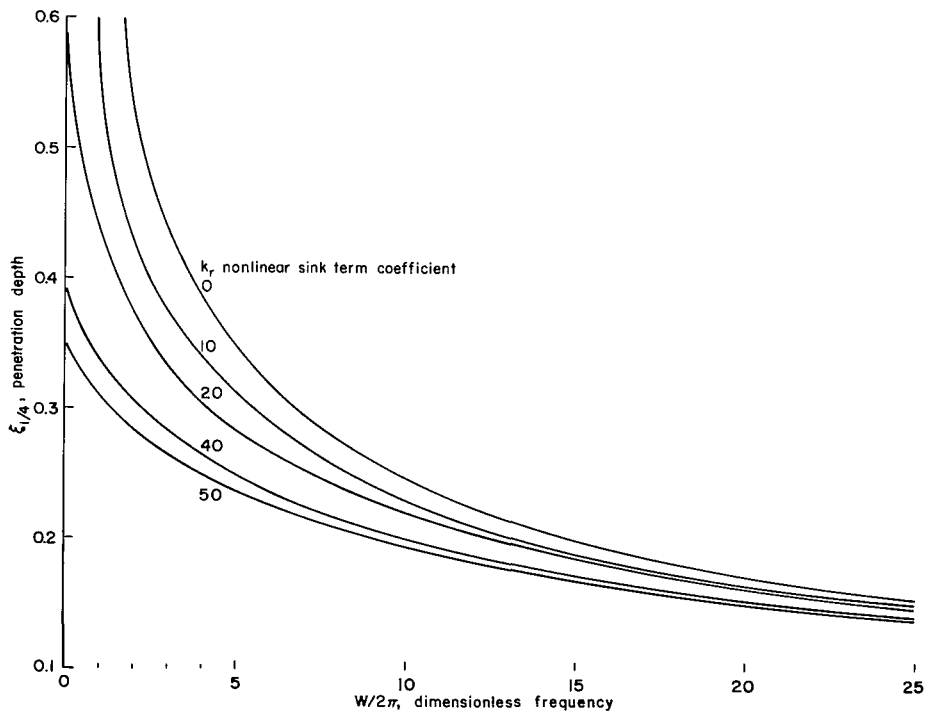


- (k) Dimensionless sink strength (k_r) = 20; (l) Dimensionless sink strength (k_r) = 20;
dimensionless frequency ($W/2\pi$) = 10. dimensionless frequency ($W/2\pi$) = 15.

Figure 3.- Concluded.



(a) Decay fraction $(E) = 1/e$.



(b) Decay fraction $(E) = 1/4$.

Figure 4.- Curves relating the depth parameter to the dimensionless frequency for various values of the nonlinear sink term coefficient k_r .

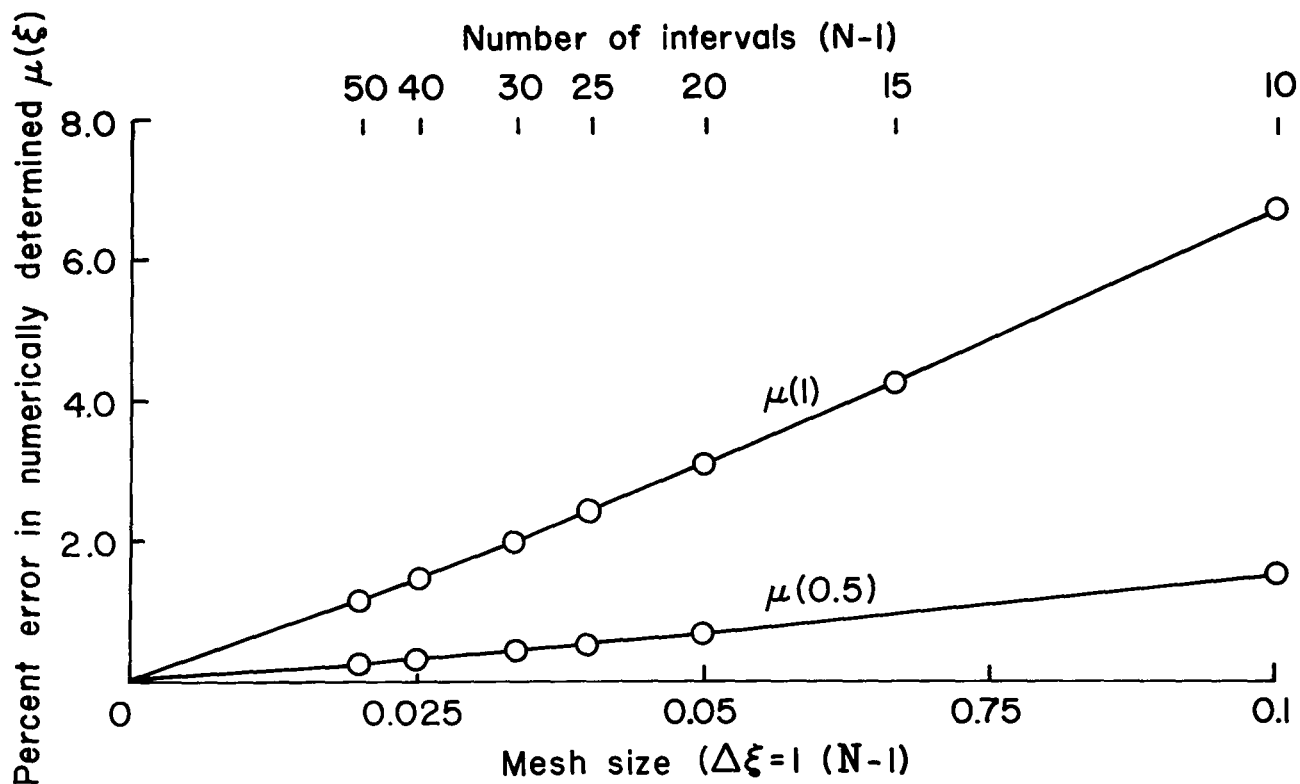


Figure 5.- Curves showing the percent error in the numerically determined steady-state solution $\mu(\xi)$ relative to equation (20) for $\xi = 1$ and $\xi = 1/2$ as a function of mesh size $\Delta\xi$. Sink strength, k_r , is 10.

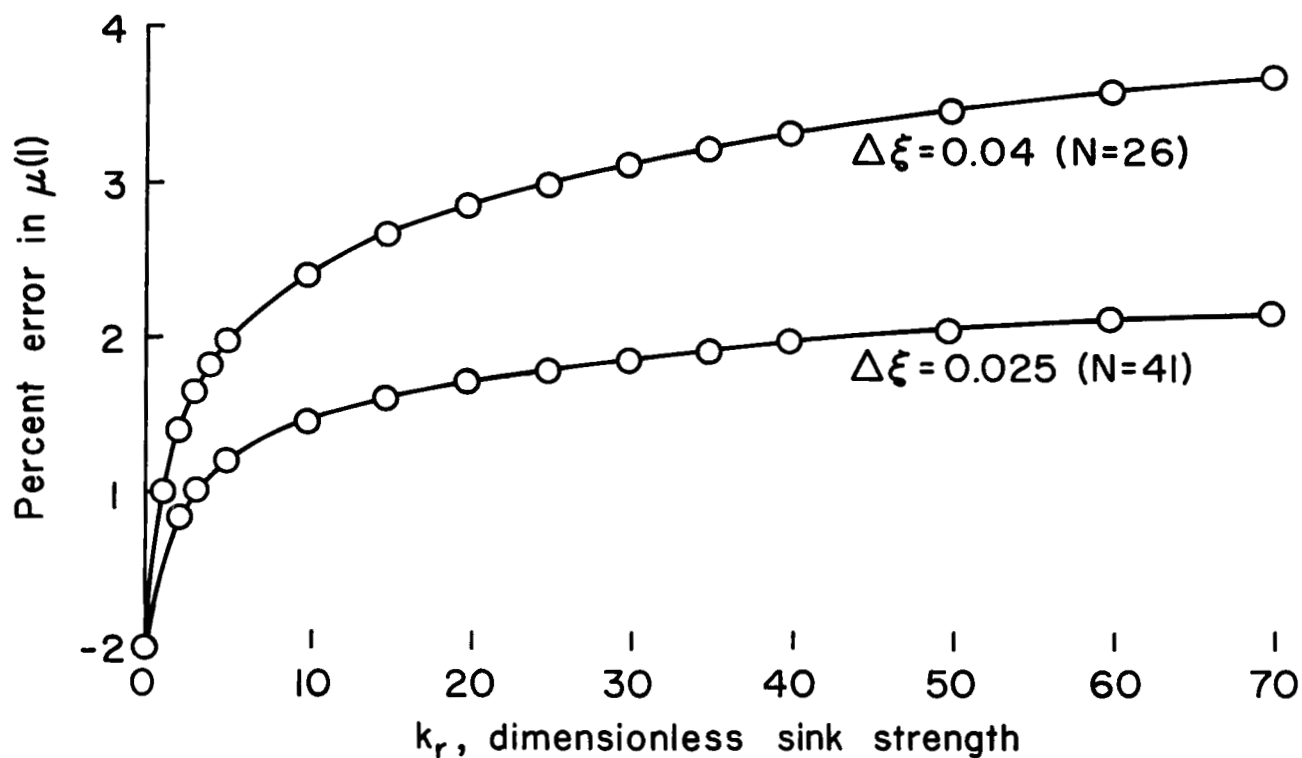


Figure 6.- Curves showing the percent error in the numerically determined far boundary value of the concentration $\mu(1)$ relative to equation (20) as a function of sink strength k_r for two specific mesh sizes, $\Delta\xi = 0.025$ and 0.04 .

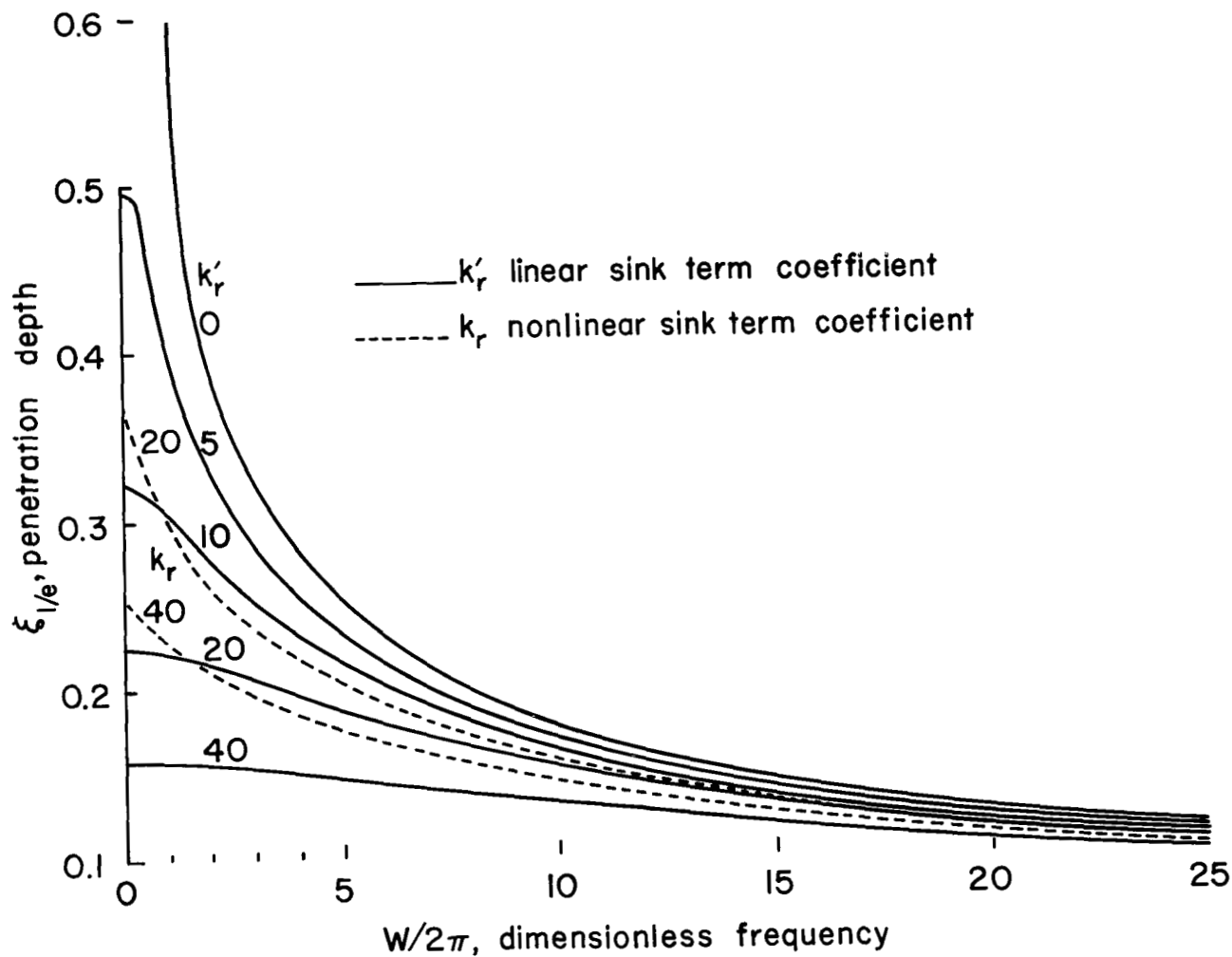


Figure 7.- Curves showing the comparison between depth parameters obtained from a linear approximation to the sink term and those obtained from the numerical solution with a nonlinear sink term.